Article

A Comprehensive Microstructural and Compositional Characterization of Allogenic and Xenogenic Bone: Application to Bone Grafts and Nanostructured Biomimetic Coatings

Gabriela Graziani [1], **Marco Govoni** [2,*], **Leonardo Vivarelli** [2], **Marco Boi** [1], **Monica De Carolis** [1], **Michele Bianchi** [3], **Enrico Sassoni** [4], **Maria Chiara Bignozzi** [4], **Gianluca Carnevale** [5], **Federico Marmi** [2], **Maria Cristina Maltarello** [6] and **Dante Dallari** [2]

1   Laboratory of NanoBiotechnology, IRCCS Istituto Ortopedico Rizzoli, Via di Barbiano 1/10, 40136 Bologna, Italy; gabriela.graziani@ior.it (G.G.); marco.boi@ior.it (M.B.); monica.decarolis2@unibo.it (M.D.C.)

2   Reconstructive Orthopaedic Surgery and Innovative Techniques–Musculoskeletal Tissue Bank, IRCCS Istituto Ortopedico Rizzoli, Via G.C. Pupilli 1, 40136 Bologna, Italy; leonardo.vivarelli@ior.it (L.V.); federico.marmi@ior.it (F.M.); dante.dallari@ior.it (D.D.)

3   Center for Translational Neurophysiology of Speech and Communication, Istituto Italiano di Tecnologia, Via Fossato di Mortara 17-19, 44121 Ferrara, Italy; Michele.Bianchi@iit.it

4   Department of Civil, Chemical, Environmental and Materials Engineering (DICAM), University of Bologna, via Terracini 28, 40131 Bologna, Italy; enrico.sassoni2@unibo.it (E.S.); maria.bignozzi@unibo.it (M.C.B.)

5   Department of Surgery, Medicine, Dentistry and Morphological Sciences with Interest in Transplant, Oncology and Regenerative Medicine, University of Modena and Reggio Emilia, via del Pozzo 71, 41124 Modena, Italy; gcarneva@unimore.it

6   Laboratory of Musculoskeletal Cell Biology, IRCCS Istituto Ortopedico Rizzoli, Via di Barbiano 1/10, 40136 Bologna, Italy; mariacristina.maltarello@ior.it

*   Correspondence: marco.govoni@ior.it

Abstract: Bone grafts and bone-based materials are widely used in orthopedic surgery. However, the selection of the bone type to be used is more focused on the biological properties of bone sources than physico-chemical ones. Moreover, although biogenic sources are increasingly used for deposition of biomimetic nanostructured coatings, the influence of specific precursors used on coating's morphology and composition has not yet been explored. Therefore, in order to fill this gap, we provided a detailed characterization of the properties of the mineral phase of the most used bone sources for allografts, xenografts and coating deposition protocols, not currently available. To this aim, several bone apatite precursors are compared in terms of composition and morphology. Significant differences are assessed for the magnesium content between female and male human donors, and in terms of Ca/P ratio, magnesium content and carbonate substitution between human bone and different animal bone sources. Prospectively, based on these data, bone from different sources can be used to obtain bone grafts having slightly different properties, depending on the clinical need. Likewise, the suitability of coating-based biomimetic films for specific clinical musculoskeletal application may depend on the type of apatite precursor used, being differently able to tune surface morphology and nanostructuration, as shown in the proof of concepts of thin film manufacturing here presented.

Keywords: bone; allograft; autograft; xenograft; calcium phosphates; ion-substituted calcium phosphates; nanostructured coatings

1. Introduction

Bone grafts and bone-based materials are widely used in orthopedic surgery in the form of blocks, granulates and cements, to replace missing bone stock and favor bone regeneration. To this aim, it is widely acknowledged that autografts can guarantee the best efficacy, but lack of availability and need for invasive withdrawal procedure limit their use [1]. For this reason, allografts, xenografts and synthetic substitutes are normally preferred in the clinical practice [2,3]. In addition, synthetic bone-based materials have been engineered to avoid the potential of human disease transmission and immunogenicity, and they have the advantage of being available in unlimited quantities, but they are normally regarded only as osteoconductive. On the other hand, bone derived from human and animal sources is commonly considered both osteoconductive and osteoinductive. In addition, based on the biomimetic principle, a material as similar as possible to the host bone is recommended to allow for the best biological behavior [4–6]. Therefore, both allografts and xenografts are extensively used. The use of bone-derived materials is raising increasing interest in the literature, also for what regards advanced biomedical devices, and in particular for particles, granulates and biomimetic coatings [7–16]. The latter are a newer application of biogenic bone, but they are raising increasing interest, thanks to the increasing capability of plasma-assisted techniques to transfer the composition of the target to the coatings, which makes deposition from biogenic sources one of the fastest and more reliable ways to obtain multi-substituted biomimetic thin films. While human, bovine, equine and, to a lower extent, porcine and ovine bone are used for the grafts and the granulates, coatings are normally obtained by animal bone (ovine and bovine bone).

However, the exact composition of bone is known to be largely dependent on several factors, such as animal species, sex of the donor, age, anatomical site, specific characteristics of the donor, possible pathologies, level of physical activity and alimentation [5,6,17–19]. Several studies focus on the characterization of bone substitutes from a mechanical point of view [20], while only few deals with the characterization of the physico-chemical properties of bone apatite deriving from different human and animal sources. The latter generally take into exam characterization of the effects of calcination or other deproteinization procedures [21–23], materials of interest for dentistry, such as animal and human teeth [24–28] or focus on goals different from medicine [29–32]. At present, to the Authors' best knowledge, no studies exist that carry out an extensive and comparative evaluation of composition of bone grafts used in the biomedical field. In fact, to date, the choice of bone substitutes is mainly based on the surgeon's experience, while understanding the physico-chemical properties of bone would allow a better selection of the most appropriate treating option. Therefore, here, we investigate the physico-chemical and morphological properties of human and animal bone to better understand their main characteristics in terms of composition and their variability, for three main aims:

- Understanding physico-chemical variability among human bone, also depending on the sex of the donor. To this aim, the main parameters influencing the behavior of biological (as well as synthetic) hydroxyapatite (HA—$Ca_{10}(PO_4)_6OH_2$)—i.e., phase composition, crystallinity, Ca/P ratio, content of magnesium—are investigated;
- Comparing the composition of human bone to that of different animal species, commonly used as bone grafts, to understand their effective similarity to host bone;
- Understanding the differences that exist between different sources and how they are translated in clinics when bone is used for biomedical devices. This is particularly relevant for coatings, where obtaining a bone-like composition and the preserving stoichiometry from the deposition target to the film is particularly challenging [6].

To this regard, compared to grafts, powders and granulates, in the coatings, plasma assisted deposition can cause significant alterations in phase composition of the starting material, including formation of decomposition phases [33]. In addition, pre/post deposition thermal treatments are commonly used to tune crystallinity, which can also cause modifications in the composition of the film. This can enhance, or mask, eventual differences between the precursors, in an unpredictable way. For this

reason, here, nanostructured coatings are manufactured starting from different animal precursors and human male/female bone, to understand if the differences in the composition of bone can be translated in differences in the achieved coatings, or can lead to the presence of metastable/decomposition phases.

Ionized Jet Deposition (IJD) is selected for the deposition, which is a plasma assisted technique, recently proposed for the development of biomimetic thin films [12]. Briefly, in IJD, a target material is ablated by a fast pulse, high energy electron beam, causing the formation of a plasma plume, that is accelerate towards a substrate, where it grows as a nanostructured thin film. Previously, the authors have demonstrated that IJD permits to transfer the exact composition of the target to the coatings, without leading to the formation of decomposition phases [7,12]. In addition, when depositing bone-apatite, transfer of trace ions is permitted, so that the films strongly resembles the composition of bone. IJD is very sensitive to the exact composition and mechanical characteristics of the targets, therefore here, the deposition of different biogenic sources is explored, to understand: (i) how the changes in the precursors impact on the characteristics of the coatings and (ii) the suitability of the use of each animal and human source.

2. Materials and Methods

2.1. Sample Collection

Human bone samples were provided by the Muskoloskeletal Tissue Bank of IRCCS Istituto Ortopedico Rizzoli (Bologna, Italy), in accordance with the approval of the Local Ethics Committee (cod. 75/17). In this study, only specimens not suitable for transplantation and considered as waste materials were used, according to the Italian law and National Transplantation Center's guidelines. From 9 human cadaveric donors, 4 male and 5 female, 11 specimens were obtained to have sufficient data while minimizing the number of samples collected. All samples were collected from the same anatomical site, by retrieving a 5 mm thick ring from the lesser trochanter, about 2 cm below the femoral epiphysis. Two femurs were found positive to microbiological controls and irradiated with gamma rays following the Tissue Bank guidelines. Literature studies indicate that significant differences arise in biological and mechanical properties of bones, following gamma irradiation [34–37]. For this reason, samples from these femurs were included in the experimentation, to preliminary assess if and how the irradiation can also cause alterations in bone composition.

Bone tissue from different animal species (ovine, bovine, porcine, equine) was compared. Three samples were selected for each animal species, based on preliminary tests aimed at evaluating variability inside each species. As for humans, for each species, all samples were taken from the same area, i.e., femoral diaphysis, so that the results could be negligent of differences caused by the anatomical site. Animal shafts were obtained by different local butchers from adult animals (age range: ovine, 8–10 months; porcine, 5–7 months; bovine, 8–12 months; equine, 12–15 months). All samples were stored at −80 °C until experimental analysis.

2.2. Sample Preparation

All human and animal samples were thawed overnight at 4 °C and then deproteinized by stirring in 2.6 wt.% solution of NaOCl in deionized water to remove the organic components [38–41].

Efficacy of deproteinization was verified by Fourier-Transform Infrared spectroscopy (FT-IR, Spectrum Two, PerkinElmer, Waltham, MA, USA) at 7, 14 and 21 days of bleaching and thermal gravimetric analysis (TGA, Q50, TA Instrument, New Castle, DE, USA) at 14 and 21 days. Based on the results, all samples were deproteinized by immersion for 14 days, except for ovine bone, for which the deproteinization process was extended up to 21 days.

Samples were labeled in semi-anonymized form by an alphanumeric code, as listed in Table 1.

Table 1. Samples for human donors. Letters F (female) or M (male) indicate the donor gender, while numbers are referred to the batch record of processed tissues. Samples indicated by the letter "γ" were subjected to sterilization with gamma rays.

Gender	Amount	Name	Median Age	Age Range
Female	7	F34, F41, F43, F46, F46γ, F78, F78γ	49.4 years	47–52 years
Male	4	M40, M45, M47, M69	57.8 years	53–60 years

Moreover, as stated above, for two donors (F46 and F78), both femurs were collected and one of each has been treated by gamma rays, as found positive to microbiological controls, according to the procedure normally followed by the Tissue Bank. The minimum validated dose for sterilization by gamma irradiation is 25 kGy, in accordance with ISO 11137-2:2013 [42]. However, this dose is usually exceeded to ensure thorough sterilization. A dosage range of 25.9–34.5 kGy was used in F46γ and F78γ, as reported in the sterility documentation provided by Sterigenics S.p.A (Bologna, Italy) and Gammatom S.r.l (Como, Italy).

2.3. Sample Characterization

Morphology and elemental composition were analyzed by a Scanning Electron Microscope (SEM, EVO/MA10, ZEISS, Oberkochen, Germany) equipped with an Energy Dispersive X-ray (EDS, INCA Energy 200, Oxford Instruments, Abingdon-on-Thames, UK). The EDS analyses were performed on three different zones of each sample and averaged. The spectrum was acquired at an operating voltage of 15 kV. Samples (1 cm × 0.5 cm × 0.5 cm) were left uncoated for the analyses.

Sample composition was assessed by Fourier transform infrared spectroscopy (FTIR-ATR, Spectrum 2, acquisition parameters: resolution 1 cm^{-1}, accumulation 64 scans, data interval 0.5 cm^{-1}, PerkinElmer, Waltham, MA, USA). Phase structure and crystallinity of the samples has been investigated by X-rays diffractometry (XRD, X'Pert PRO, Malvern Panalytical, Malvern, UK, $\varphi = 5°–80°$, scan step size 0.017°, time per step 50 s). XRD data were filtered (five-point linear averaging) using the Matlab software (v. R2014b, MathWorks, Natick, MA, USA) to obtain a better graphic representation.

Both FT-IR and XRD were carried out on powders, obtained by manually grinding the samples in an agate mortar.

To highlight differences between the samples, all FT-IR spectra were scaled with respect to the band at 1030 cm^{-1} (phosphate stretching). By doing so, differences in relative amount of phases that constitute the samples (e.g., carbonates vs. phosphates, metastable phases/hydroxyapatite) can be qualitatively evaluated. All XRD spectra were scaled with respect to the peak at $2\theta = 31.7°$ (peak intensity 100% of hydroxyapatite), which is the main peak for all the examined spectra. By doing so, possible differences in the phase composition of the samples (i.e., presence of soluble phases alongside hydroxyapatite), could be qualitatively detected.

Based on these tests, the following parameters were assessed, all being crucial into determining the solubility of biogenic apatite and the type and amount of ions released in the peri-implant environment:

- Ca/P ratio (EDS);
- Magnesium content (EDS);
- Carbonate content (FT-IR);
- Presence/absence of metastable phase different from hydroxyapatite (FT-IR, XRD);
- Crystallinity (XRD).

2.4. Coatings Manufacturing and Characterization

Biomimetic bone apatite coatings have been recently proposed by the authors [8,12], manufactured by an Ionized Jet Deposition (IJD). Here, deposition from different sources is compared.

For deposition of the biomimetic coatings, bone from each source is deproteinized, as described above, to remove organic traces that could hamper coatings uniformity and/or adhesion to the substrate.

Then, they are shaped in the form of disks (2.5 cm diameter, 5 mm thickness), suitable for IJD deposition. After shaping, the disks are mounted on rotating holders in the deposition chamber, to ensure uniformity of deposition. Here, silicon wafers are used as substrates, as they permit a better evaluation of coatings morphology, being atomically flat. Deposition is carried out at room temperature, in the very same way for each precursor, i.e., keeping all deposition parameters constant (substrate-target distance, voltage, frequency, deposition time). Based on preliminary results obtained for bovine bone [7,8], the following deposition parameters are selected: substrate-target distance 8 cm, voltage 18 kV, frequency 7 kHz, deposition time 30 min. Substrate-target distance is selected to ensure uniformity in depositions on the samples, while voltage and frequency must allow optimal ablation and formation of a plasma plume at each pulse of the electron beam. Deposition time, instead, determines film thickness, here corresponding to about 450 nm thickness. This thickness was selected based on the optimization of adhesion to substrate, absence of cracks and delamination and based on in vitro tests on dental pulp stem cells [8]. After deposition, all coatings are annealed for 1 h in air at 400 °C, to tune crystallinity up to resembling that of bone.

After deposition, morphology (SEM) and composition (FT-IR) of the films are examined to detect differences in morphology and/or composition between the different films.

2.5. Statistical Analysis

Statistical analysis is performed using GraphPad Prism ver. 6 (http://www.graphpad.com). EDS data are expressed as mean ± standard deviation and comparison between groups is performed using the two-tailed, unpaired Student's *t*-test. Differences are considered significant for $p < 0.05$.

3. Results

3.1. Human Specimens

3.1.1. Bone Morphology

Human specimens have been characterized in terms of morphology, as shown in Figure 1. For clarity's sake, only a part of the samples is reported in Figure 1, while SEM images for all specimens are in the Supplementary Material, Figures S1 and S2.
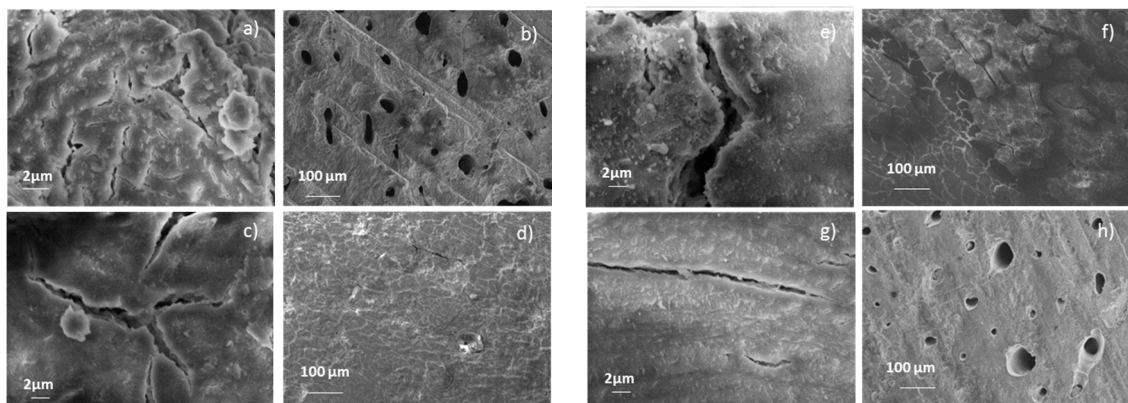

Figure 1. SEM images of representative female and male donor bone samples: F34 (**a**,**b**), F41 (**c**,**d**), M40 (**e**,**f**), M45 (**g**,**h**).

Significant differences are found concerning the morphology of bone samples, as variable amount, dimension and shape of pores are found between different specimens, though not correlated to donor gender. Although mercury intrusion porosimetry would be needed to quantify total open porosity and pore size distribution, a qualitative evaluation can be already obtained by SEM images, as the differences between different samples are significant and highly reproducible.

3.1.2. Phase and Elemental Composition

Phase composition has been investigated by FT-IR and XRD. Results are in Figure 2a,b, respectively.
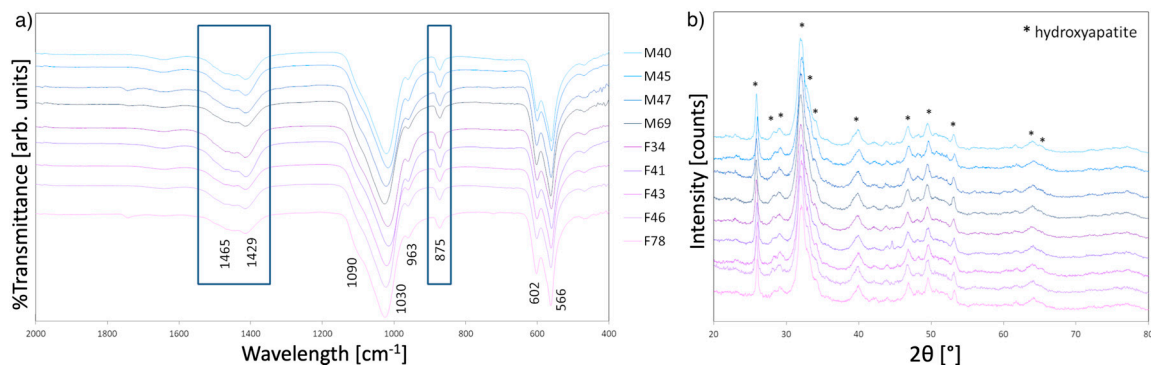
Figure 2. Composition of human bone samples: (**a**) FT-IR and (**b**) XRD spectra. Bands characteristic of CHA (1465, 1429, 875 cm^{-1}) [43,44] and HA (1090, 1030, 963, 602, 566 cm^{-1}) [45,46] are detected in FT-IR graphs, while all peaks detected in XRD patterns are characteristic of hydroxyapatite.

FT-IR spectra exhibit bands characteristic of hydroxyapatite and carbonated hydroxyapatite [43–46]. All samples exhibit bands at 1465, 1429 cm^{-1} (asymmetrical and symmetrical stretching modes of $CO_3\nu_3$), 870 cm^{-1} ($CO_3\nu_2$), 1030 cm^{-1} (antisymmetric stretching mode ν_3PO_4), 963 cm^{-1} (ν_1PO_4 symmetric stretch), 602 and 566 cm^{-1} (ν_4PO_4 antisymmetric bend), 469 cm^{-1} (ν_2PO_4 bend).

FT-IR spectra evidence a non-negligible variability in the amplitude of carbonate bands (1465, 1429, 870 cm^{-1}) compared to phosphates (1030 cm^{-1}) between different human donors. This could be ascribed to a different level of carbonate substitutions in the samples. On the other hand, no significant differences are evidenced between bone deriving from female and male donors.

XRD spectra exhibit peaks characteristic of scarcely crystalline hydroxyapatite. No bands relative to octacalcium phosphate (OCP, $Ca_8H_2(PO_4)_6 \cdot 5H_2O$) or other metastable calcium phosphate phases are detected.

In addition, no differences are assessed between the composition of the different samples, regardless sex and age of the donors.

Elemental composition of human specimens has been investigated by EDS and results are summarized in Table 2. Sodium and chloride ions are neglected because could suffer alterations due to deproteinization procedure in NaOCl.

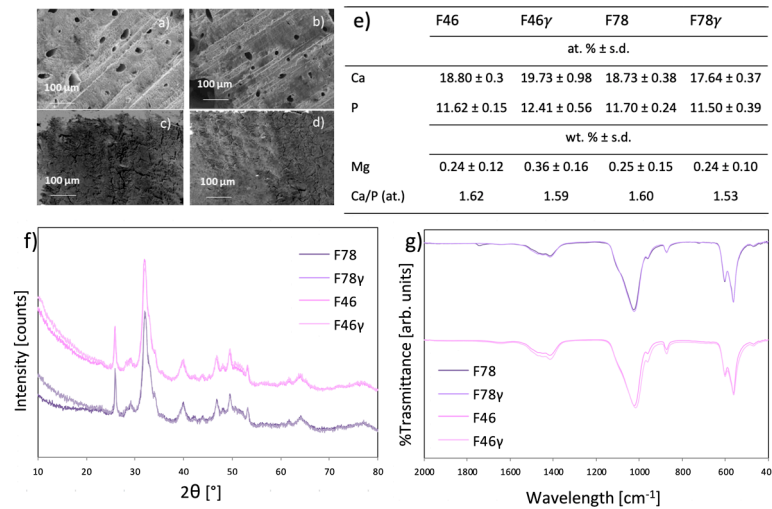**Table 2.** EDS elemental composition of human bone specimens.

Element	F43	F34	F46	F78	M45	M69	M47	M40
	at.%	at.%	at.%	at.%	at.%	at.%	at.%	at.%
Ca	18.61 ± 0.34	20.29 ± 1.41	18.80 ± 0.30	18.78 ± 0.38	17.04 ± 0.23	19.72 ± 0.84	17.57 ± 1.05	19.02 ± 1.08
P	11.47 ± 0.7	12.43 ± 0.75	11.62 ± 0.16	11.70 ± 0.24	11.08 ± 0.11	12.43 ± 0.35	10.19 ± 1.32	11.40 ± 0.30
Ca/P(at.)	1.62	1.63	1.62	1.6	1.54	1.58	1.72	1.67
Element	**wt.%**	**wt.%**	**wt.%**	**wt.%**	**wt.%**	**wt.%**	**wt.%**	**wt.%**
Ca	33.40 ± 0.54	35.48 ± 1.78	33.65 ± 0.41	33.31 ± 0.62	31.17 ± 0.35	34.62 ± 1.12	31.64 ± 1.43	33.95 ± 1.54
P	15.91 ± 0.93	16.81 ± 0.69	16.07 ± 0.24	16.09 ± 0.30	15.66 ± 0.19	16.88 ± 0.34	14.17 ± 1.62	15.74 ± 0.42
Mg	0.30 ± 0.08	0.22 ± 0.02	0.24 ± 0.12	0.25 ± 0.15	0.33 ± 0.11	0.39 ± 0.15	0.26 ± 0.16	0.37 ± 0.18
Element	**All Female wt.% ± s.d.**				**All Male wt.% ± s.d.**			
Mg	0.26 ± 0.10				0.34 ± 0.14			
Ca/P(at.)	1.62 ± 0.01				1.63 ± 0.08			

Human bone exhibits relevant differences in terms of trace content of magnesium ions, as also indicated by the high values of standard deviation. To this regard, a significant difference ($p = 0.0436$) is highlighted between female donors and male donors, the latter exhibiting a high content of magnesium.

Ca/P ratio, instead exhibits negligible variations between female and male donors, although the latter have higher internal variability.

3.1.3. Gamma Irradiation Effect

The effect of gamma irradiation on morphology and composition of two human bone specimens has also been investigated, and results are reported in Figure 3.


e)	F46	F46γ	F78	F78γ
	at. % ± s.d.			
Ca	18.80 ± 0.3	19.73 ± 0.98	18.73 ± 0.38	17.64 ± 0.37
P	11.62 ± 0.15	12.41 ± 0.56	11.70 ± 0.24	11.50 ± 0.39
	wt. % ± s.d.			
Mg	0.24 ± 0.12	0.36 ± 0.16	0.25 ± 0.15	0.24 ± 0.10
Ca/P (at.)	1.62	1.59	1.60	1.53

Figure 3. Representative SEM images of human samples F46 (**a**), F46γ (**b**), F78 (**c**), F78γ (**d**) and (**e**) EDS elemental composition, (**f**) FT-IR and (**g**) XRD spectra of the irradiated and not irradiated samples.

Gamma irradiation results in an increase in samples fragility, causing a significant mass loss. This significantly alters morphology at the macro-scale. However, morphology at the microscale (SEM) is not affected by the process. Quite alterations are present in sample composition in terms of magnesium content and Ca/P ratio. Instead, phase composition remains substantially unaltered.

### 3.2. Animal Specimens

3.2.1. Bone Morphology

Animal bone morphology is shown in Figure 4. First, animal bone exhibits a significant difference in morphology, depending on the animal species. For instance, ovine bone is much less compact than bovine and equine bone (Figure 4g,h).
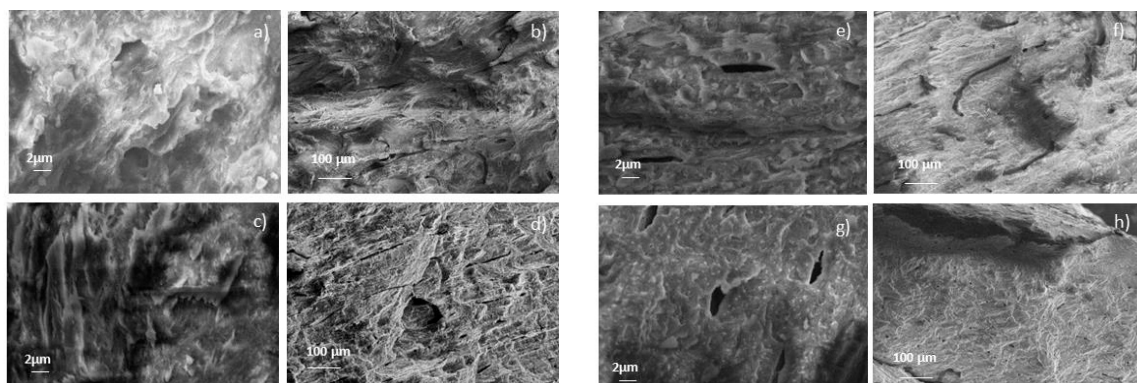
Figure 4. SEM images of bovine bone (**a**,**b**), porcine bone (**c**,**d**), equine bone (**e**,**f**) and ovine bone (**g**,**h**). Right (magnitude = 200×), left (magnitude = 5000×).

3.2.2. Phase and Elemental Composition

Animal bone composition is shown in Figure 5. Only two spectra are reported for each animal species, i.e., those exhibiting the most marked differences (for FT-IR, the spectra having the carbonates bands of lowest and highest intensity, for XRD those exhibiting the main differences in the intensity of secondary peaks).

(a)　　　　　　　　　　　　　　　　　　　　　(b)
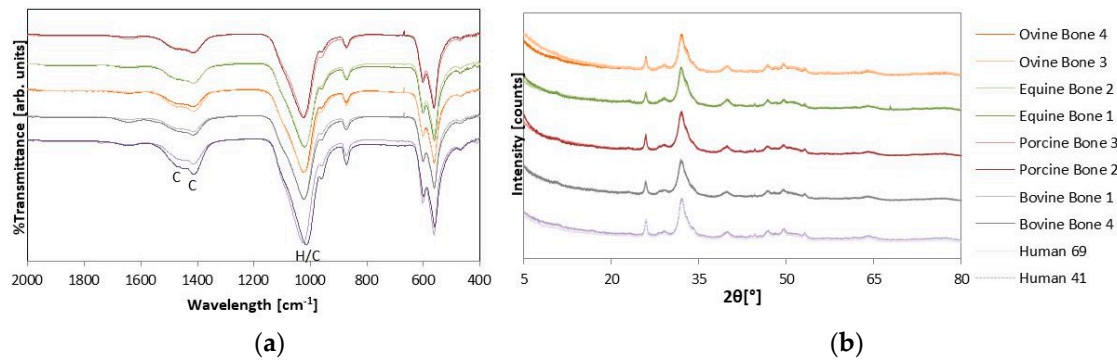
Figure 5. (**a**) FT-IR spectra of the animal and human precursors: bands characteristic of CHA (1455, 1419, 875 cm^{-1}) [43,44] and HA (1090, 1030, 600, 570 cm^{-1}) [45,46] and HA (1090, 1030, 963, 602, 566 cm^{-1} [47,48] are detected); (**b**) XRD patterns of the animal and human precursors: all peaks detected are characteristic of hydroxyapatite.

All samples exhibit almost the same phase composition, regardless of the animal source. As reported in Figure 5, the content of carbonate is lower for bovine bone. On the other hand, content of magnesium is maximum for bovine and ovine and minimum for equine (Table 3), showing a significant difference between ovine vs. equine ($p = 0.0173$) and bovine vs. equine ($p = 0.0018$). No significant differences are assessed when porcine bone is compared to the other animal sources.

Table 3. Differences in EDS elemental composition (at.% and wt.% with standard deviation, s.d.) between animal and human samples.

Element	Equine Bone	Ovine Bone	Porcine Bone	Bovine Bone	Human
	at.% ± s.d.	at.% ± s.d.	at.% ± s.d.	at.% ± s.d.	at.% ± s.d.
Ca	17.01 ± 3.06	17.43 ± 3.13	18.24 ± 3.82	16.50 ± 5.15	18.80 ± 1.23
P	10.87 ± 0.68	11.49 ± 2.05	11.78 ± 1.78	10.49 ± 0.98	11.58 ± 0.89
Element	**wt.% ± s.d.**	**wt.% ± s.d.**	**wt.% ± s.d.**	**wt.% ± s.d.**	**wt.% ± s.d.**
Ca	31.07 ± 3.78	31.61 ± 4.44	31.55 ± 5.24	30.06 ± 7.14	33.52 ± 1.66
P	15.41 ± 0.63	15.51 ± 0.98	16.29 ± 1.68	14.98 ± 1.51	15.96 ± 1.04
Mg	0.33 ± 0.02	0.64 ± 0.07	0.47 ± 0.07	0.57 ± 0.02	0.29 ± 0.02
Ca/P (at.%)	1.56	1.52	1.55	1.57	1.62

Regarding crystallinity, although slight not significant differences are appraised between specimens, Ca/P ratio is lower for ovine bone (Table 3).

3.3. Coatings Characterization

All bone sources were deposited and thermally treated, then films were analyzed in composition pre and post thermal treatment and morphology post thermal treatment.

Results show that deposition can be carried out by all the examined sources, without any significant drawback, even though easiness of shaping and target duration are bigger for bovine and equine bone.

All as-deposited coatings (Figure 6a) are highly amorphous, negligent of the deposition target. As a consequence of thermal treatments (Figure 6b), crystallinity increases for all, in a similar way, up to resembling that of real bone.
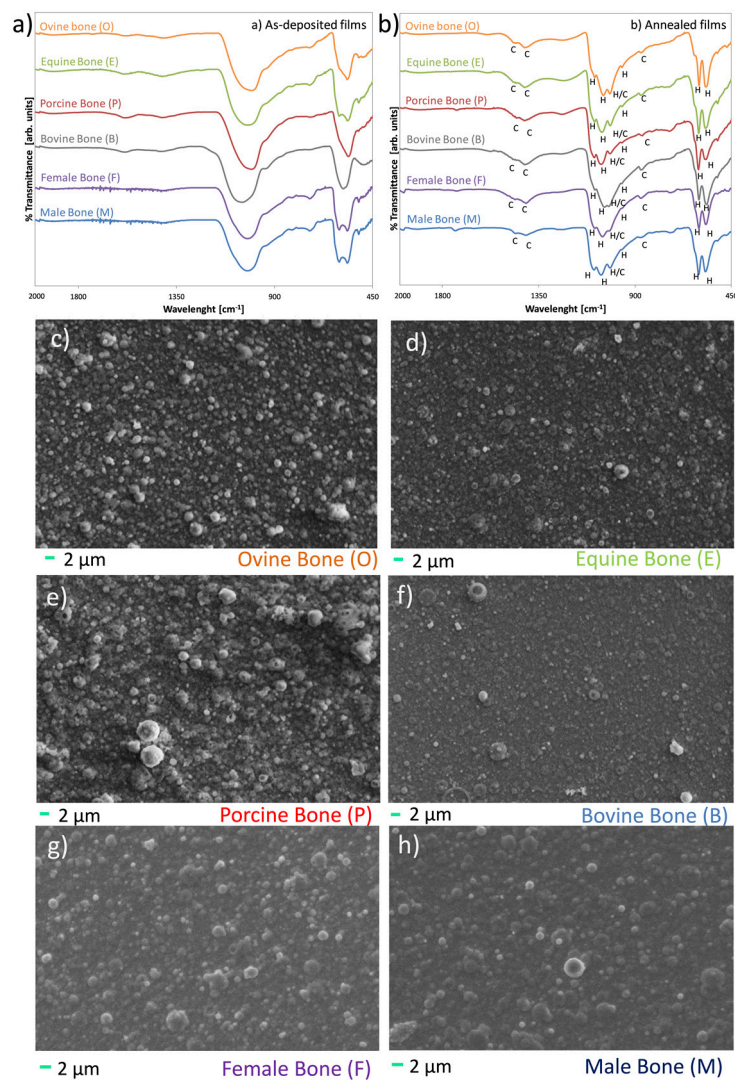
Figure 6. Composition of the coatings before (**a**) and after (**b**) thermal treatment. (**c–h**) Morphology of the coatings deposited from different sources. All as-deposited coatings are amorphous, as demonstrated by the broad and ill-defined shape of the bands in the area 1000–1500 and 560–600 cm^{-1}.

All coatings are composed by carbonated hydroxyapatite and no metastable or decomposition phases are assessed for any of the deposited films, indicating that all sources can be used for manufacturing of biomimetic films.

Morphology of the films (Figure 6c–h), instead, significantly depends on the deposition target characteristics, as more compact and harder bone result in finer aggregates and more homogeneous films.

4. Discussion

Bone grafts and substitutes are significantly used to treat bone defects and local bone loss. It is estimated that in the US, approximately 500,000 bone graft procedures are performed annually [49]. Moreover, the increasing number of musculoskeletal conditions such as osteoarthritis, rheumatoid arthritis, osteoporosis, osteopenia and traumatic fractures is a leading factor to further stimulate the global bone grafts and substitutes market over the years.

Ideally, a bone graft should have some biological properties such as the absence of immunogenicity, rapid incorporation and stable fixation capability. In addition, it should mediate recruitment of mesenchymal stem cells derived from host site (osteoinduction) and promote the bone growth on its surface or down into pores, channels or pipes (osteoconduction). Finally, some clinical particularities

such as cost-effectiveness, indefinite storage capability and easy handling properties are needed. To date, each type of bone graft has its own unique advantages and disadvantages and the relationship between bone healing and various aspects of biological, mechanical and compositional properties should be well-considered.

Among the available grafts, although autografts are still considered as the gold standard since all biological properties in terms of bone regeneration are exhibited, the concerns of limited supply and donor site complications limit their use. This is a clear indication that the use of alternative bone grafting is often necessary. Thus, allografts, xenografts and synthetic substitutes are normally preferred in the clinical practice. However, synthetic bone-based materials are normally regarded only as osteoconductive. In addition, as reported above, a material as similar as possible to the host bone is recommended to allow for the best biological behavior [4–6]. As a consequence, both allografts and xenografts are extensively used despite it is still not clear which is better for clinical purposes, because opposing results have been reported. In fact, despites some authors demonstrated that allografts outperform xenografts, others showed no significantly different outcomes.

As an example, Cook et al. [50] asserted that xenograft implantation was avoided in the past in foot and ankle surgery because of concerns about antigenicity and graft rejection, suggesting that advances in processing and sterilization techniques are needed in order to reduce immunogenicity. In 2015, Shibuya et al. [2] compared incorporation rate of allograft with bovine-based xenograft. Results showed that bovine bone was not adequate for the purpose of foot and ankle reconstructive surgery in both union rate and incorporation time. Sousa et al. [51] investigated the osteoconduction and bioresorption properties of bone allograft vs. anorganic bovine xenograft by a histomorphometric study in humans. Volume density of connective tissue was similar between groups, although greater osteoconductivity and faster bioresorption were noticeable in the allograft group. Recently, Rhodes et al. [52] compared the use of bovine xenograft and cadaveric allograft for calcaneal lengthening osteotomy in patients with cerebral palsy. Authors affirmed that allograft incorporated better than xenograft, yet both groups retained postoperative improvement.

In addition, whilst many studies focus on the allografts and xenografts based on their biological or mechanical [53–55] properties, there is a lack of information regarding the physico-chemical properties of bone apatite deriving from different human and animal sources. Instead, the properties of the mineral phase of bone can significantly impact on its biological behavior as trace ions incorporated in the lattice change the solubility of hydroxyapatite and can have important therapeutic effects (as in the case of magnesium). As a consequence, the use of hydroxyapatites with different type/amount of substitutions results in a different type and concentration of ions released in the peri-implant environment, which in turn, significantly influences the biological behavior of the graft. Lack of similarity between stoichiometric and biological apatite, in fact, is among the main reasons of the scarce behavior of hydroxyapatite-based materials, and in particular of coatings [5,6,33,56].

Stoichiometric HA is basically composed of calcium and phosphorus with molar ratio of Ca/P equal to 1.67 [57]. This ratio has been proven to be the most effective in promoting bone regeneration [30]. However, the mineral component of bone is a non-stoichiometric hydroxyapatite with trace amounts of ions such as Na^+, Mg^{2+} and Al^{3+} substituted in the calcium positions. The trace elements are essential in the regeneration of the bone and accelerates the process of bone formation. Moreover, carbonate is present in biological apatites by substitution at phosphate and hydroxide sites, tending to increase its solubility and the amount of in vivo osseointegration in comparison with pure hydroxyapatite [58].

As shown in Figure 2a,b, FT-IR and XRD analyses have not reported significant differences between human samples regarding both the age and sex of the donors. Specifically, FT-IR spectra highlighted a non-negligible variability in the amplitude of carbonate bands compared to phosphates, while XRD spectra showed peaks characteristic of a scarcely crystalline HA. These differences in crystallinity between stoichiometric and biogenic apatite are significant, as stoichiometric apatite would be essentially insoluble at the pH ranges present in the human body, also in the case of inflammation.

Although information about the elemental composition obtained by EDS analysis (Table 2) exhibited slight variation between female and male donors, they highlighted a significant difference in terms of magnesium trace ($p < 0.05$). In particular, male donors displayed the higher content. Magnesium has an important role on hydroxyapatite crystal and a significant biological relevance. In fact, it causes a decrease in the c-axis of the lattice, acting like a suppressor for HA nucleation and crystallization and destabilizing the apatitic structure [5,6,13,19]. Mg-substitutions make HA less crystalline, therefore its solubility increases. From a biological point of view, magnesium is an essential element for living organisms, as it is a co-factor for over 100 enzymes, influences the metabolic activity and growth of bone by acting on osteoblasts and osteoclasts activity [5,6,13,19]. As a consequence, even though a composition as similar as possible to the host bone is recommended based on the biomimetic principle, magnesium is frequently added in biomaterials in concentrations higher than those of bone [6], to improve its biological behavior and increase the dissolution rate. As a consequence, a high level of magnesium can be preferred; thus, for regenerative medicine intent, male donors may be preferred since the high content of magnesium makes this bone material more degradable and resorbable, in order to be replaced gradually by the new bone after implantation. Obviously, bone regeneration quality is decided by many factors, despite the in vitro solubility of the graft is an important parameter in the evaluation of its biodegradability and in vivo performance.

Therefore, these data highlight the need, that is increasingly emerging in the Literature, for specific in vitro and in vivo studies based on the donor's gender. More attention should be paid for female that are commonly neglected in clinical studies in orthopedics, that tend to take into exam tissues deriving from male donors only. This also indicates that specific biomaterials and grafts (both synthetic and from biogenic sources) could be addressed to male and female patients. A characterization of differences in soft tissues between male and female donors could be of interest as well.

When morphology of human and animal specimens is compared (SEM, Figures 1 and 4), significant differences are assessed regarding variation between the species and within one same species. In fact, human bone has shown a more marked morphological heterogeneity, especially about porosity, than animal sources. A higher porosity results in scarcer mechanical properties, but also in increased specific surface and higher host cells adhesion and proliferation. As a consequence, porosity and morphology shall be taken into consideration when selecting a graft.

As expected, also animal bone exhibits a significant difference in morphology between different species. Specifically, bovine and equine bone is more compact than the other specimens and appears scarcely porous, although more detailed analyses must be carried out to investigate this point. This suggests that bovine bone and equine is more adequate for grafts of medium-big dimensions, as higher porosity results in scarcer mechanical properties, but could be less prone to dissolution and to favoring cells adhesion.

When compared to human bone, all specimens within one same species exhibit a much lower variability in phase-composition. In addition, FT-IR and XRD spectra and EDS (Figure 5 and Table 3) indicate that differences exist in terms of all the investigated parameters. First, on average, the content of carbonates is maximum for human bone (FT-IR) and lower for animal specimens, especially for bovine bone. On the other hand, content of magnesium is significantly higher for ovine, bovine and porcine bone as compared to human bone ($p = 0.002$, $p = 0.0001$, $p = 0.0122$, respectively). No statistical difference is assessed between equine and human bone. Regarding Ca/P ratio, although slight differences are appreciated when human and animal sources are compared, the maximum value (closer to stoichiometric value of HA) is assessed for human bone and minimum for ovine. Bovine, equine and porcine bone exhibit similar Ca/P ratio.

Regarding crystallinity, negligible differences are assessed between the specimens, although crystallinity is maximum for human bone, consistently with Ca/P ratio. In addition, no appreciable differences are assessed in the dimension of crystallites, different from what was reported in some literature data [47,48].

This indicates that different animal sources can be used to address different aims: (i) a higher or lower content of magnesium can be selected depending on therapeutic needs and/or patient gender; (ii) a bone with higher or lower Ca/P ratio can be used to achieve faster or slower dissolution rate; (iii) a greater porosity can be selected to facilitate cell infiltration and adhesion through the 3D environment; (iv) when specific mechanical properties, such as compressive strength and shear force resistance are needed, a more compact bone structure could be indicated.

These considerations are not only valid for bone grafts, but for any bone-based or biomimetic biomaterial.

A detailed in vitro characterization is currently in progress to determine how these differences translate into a modulation of host cell behavior.

In addition, preliminary results on the effect of gamma irradiation on human female samples show quite significant alterations in terms of magnesium content and Ca/P ratio, possibly correlated to material loss. On the other hand, phase composition remains substantially unaltered suggesting that gamma irradiation does not cause alterations in bone tissue composition, that could affect its biological behavior, but causes a significant reduction in processability, given by increased fragility and tendency to pulverization, possibly leading to inflammation. Obviously, a more detailed characterization, based on an increased number of samples is suggested, to also include male donors.

The reported data, summarized in Table 4, provide information beside the published scientific papers in the literature regarding allograft and xenograft composition but do not address certain issues, such as indications, specifications, dosage, limitations and contraindications of bone grafts and substitutes. The goal of achieving an optimal bone-implant interface should be approached considering several parameters such as implant surface topography, chemistry, bulk material composition, resistance in the physiologic milieu, acceptable strength [59]. Nevertheless, these results may be considered, together with biological and mechanical properties of different bone sources, as the basis to design multicenter prospective randomized studies focused on the choice of the most appropriate graft for a specific clinical application.

Table 4. Overview of the main characteristics of the investigated specimens. All values are compared to male human bone (reference), and differences are visually indicated in terms of sign (higher/lower/similar: +/−/≈) and magnitude (+/++, −/− −).

Element	Human Male	Human Female	Human Female γ	Equine	Ovine	Porcine	Bovine
Mg	ref	−	−	≈	++	+	+ +
Ca/P	ref	≈	−	− −	− −	− −	−
Carbonates substitution	ref	≈	≈	−	− −	−	− −

When bone from different sources are used to manufacture nanostructured coatings, they all allow achieving nanostructured biomimetic thin films. All deposited films are highly amorphous, but crystallinity can be tuned by post treatment annealing. All coatings are constituted by ion-doped carbonated hydroxyapatites, whose composition closely resembles that of the relevant deposition targets. However, differences in the composition of the films are negligible, thus indicating that initial differences between bone specimens are less important than the alterations caused in composition by the deposition procedure and by thermal treatment. In particular, if results obtained here are compared with previous results from the Authors [12], it is clear that: (i) plasma deposition causes modifications in the Ca/P ratio, which are more significant than those present between bone from different sources and (ii) annealing temperature has a much stronger impact on the content of carbonates than bone source does.

Similarly, because phase composition is substantially the same for all samples, no differences are assessed in the behavior of the films with respect to annealing. In fact, similar increases in crystallinity are observed in the same temperature range, as demonstrated by the narrowing of bands in IR spectra, while no cracking/spalling phenomena are observed for any of the coatings, as a result of heating.

Instead, different precursors allow achieving significantly different surface morphology and nanostructuration, where more compact bone (equine and bovine) permits a more regular morphology constituted by finer aggregates, while softer bone allows achieving coarser but more irregular aggregates. A similar behavior had been observed comparing ceramics with significantly different properties [60], but results achieved here show that slight alterations in the target morphology can be successfully exploited to tune morphology and in turn, specific surface, which determines ion release. This is important as it has been demonstrated that macro-, micro- and, mostly, nano-sized topographical cues can stimulate changes at cellular and tissue level [61]. For this reason, an increasing number of studies investigate surface patterning and tuning of nanostructuration and materials surface roughness to direct cells adhesion and osteogenic differentiation [62]. For nanostructured thin films, Literature studies are being devoted to modifying the shape, orientation and dimensions of the aggregates to tune cells response, for example by applying glancing angle deposition [63]. Here we demonstrate that the characteristics of the target also have a strong importance on the morphological outcome of deposition and can be exploited for a simple and fast tuning of the micro- and nano-structure of the coatings.

5. Conclusions

In this paper, different bone sources are studied and compared to assess possible differences from a compositional point of view.

Although all samples are composed by the same main inorganic phase (carbonated, multi-substituted hydroxyapatite), significant differences are assessed between female and male human samples and between animal and human bone, especially for what regards the content of magnesium, and slight differences in terms of carbonate substitution and Ca/P ratio. These parameters are known to influence solubility and ion release from the different sources, hence could have an impact on the behavior of bone substitutes. Although ovine, porcine and bovine have a greater content of magnesium with respect to human bone, they exhibit scarce similarity to human bone in terms of carbonates content and Ca/P ratio. Thus, although every bone material may have different clinical applications depending on the expected effect that the clinician demands, human bone from male donors emerge as more appropriate for regenerative purposes. In addition, differences existing between biogenic apatite from human and animal bone could be among the reasons allowing a better performance for allografts compared to xenografts, especially when a faster osseointegration is needed. In addition, significant differences assessed in the physico-chemical composition of female and male bone, should push towards a more detailed investigation of gender-specific studies, also to understand gender disparities in some chronic and degenerative musculoskeletal pathologies such as osteoarthritis and osteoporosis.

Finally, bone from different biogenic sources can be successfully used to manufacture biomimetic thin films, having a nanosized surface roughness and a composition strongly resembling that of bone. Negligent of the deposition target, post-treatment annealing at 400° permits to convert highly amorphous coatings, into films having a crystallinity similar to that of bone.

The results presented here indicate that the selection of the animal precursor to be used for the coatings shall be selected based on the desired morphology, rather than to obtain differences in coatings composition. Most importantly, differences in the mechanical properties of the targets permit to tune surface morphology and nanostructuration of the films, obtaining aggregates of different dimensions and uniformity, thus appearing as a potentially promising tool, to tune host cells adhesion and differentiation.

References

1.　Ricciardi, B.F.; Bostrom, M.P. Bone graft substitutes: Claims and credibility. *Semin. Arthroplast.* **2013**, *24*, 119–123. [CrossRef]

2.　Shibuya, N.; Jupiter, D.C. Bone graft substitute: Allograft and xenograft. *Clin. Podiatr. Med. Surg.* **2015**, *32*, 21–34. [CrossRef] [PubMed]

3.　Campana, V.; Milano, G.; Pagano, E.; Barba, M.; Cicione, C.; Salonna, G.; Lattanzi, W.; Logroscino, G. Bone substitutes in orthopaedic surgery: From basic science to clinical practice. *J. Mater. Sci. Mater. Med.* **2014**, *25*, 2445–2461. [CrossRef] [PubMed]

4.　Barinov, S.M.; Rau, J.V.; Fadeeva, I.V.; Cesaro, S.N.; Ferro, D.; Trionfetti, G.; Komlev, V.S.; Bibikov, V.Y. Carbonate loss from two magnesium-substituted carbonated apatites prepared by different synthesis techniques. *Mater. Res. Bull.* **2006**, *41*, 485–494. [CrossRef]

5.　Boanini, E.; Gazzano, M.; Bigi, A. Ionic substitutions in calcium phosphates synthesized at low temperature. *Acta Biomater.* **2010**, *6*, 1882–1894. [CrossRef]

6.　Graziani, G.; Bianchi, M.; Sassoni, E.; Russo, A.; Marcacci, M. Ion-substituted calcium phosphate coatings deposited by plasma-assisted techniques: A review. *Mater. Sci. Eng. C Mater. Biol. Appl.* **2017**, *74*, 219–229. [CrossRef]

7.　Bianchi, M.; Gambardella, A.; Graziani, G.; Liscio, F.; Maltarello, M.C.; Boi, M.; Berni, M.; Bellucci, D.; Marchiori, G.; Valle, F.; et al. Plasma-assisted deposition of bone apatite-like thin films from natural apatite. *Mater. Lett.* **2017**, *199*, 32–36. [CrossRef]

8.　Bianchi, M.; Pisciotta, A.; Bertoni, L.; Berni, M.; Gambardella, A.; Visani, A.; Russo, A.; de Pol, A.; Carnevale, G. Osteogenic differentiation of hDPSCs on biogenic bone apatite thin films. *Stem Cells Int.* **2017**, *2017*, 3579283. [CrossRef]

9.　Duta, L.; Mihailescu, N.; Popescu, A.C.; Luculescu, C.R.; Mihailescu, I.N.; Cetin, G.; Gunduz, O.; Oktar, F.N.; Popa, A.C.; Kuncser, A.; et al. Comparative physical, chemical and biological assessment of simple and titanium-doped ovine dentine-derived hydroxyapatite coatings fabricated by pulsed laser deposition. *Appl. Surf. Sci.* **2017**, *413*, 129–139. [CrossRef]

10.　Duta, L.; Oktar, F.N.; Stan, G.E.; Popescu-Pelin, G.; Serban, N.; Luculescu, C.; Mihailescu, I.N. Novel doped hydroxyapatite thin films obtained by pulsed laser deposition. *Appl. Surf. Sci.* **2013**, *265*, 41–49. [CrossRef]

11.　Duta, L.; Serban, N.; Oktar, F.N.; Mihailescu, I.N. Biological hydroxyapatite thin films synthesized by pulsed laser deposition. *Optoelectron. Adv. Mater. Rapid Commun.* **2013**, *7*, 1040–1044.

12.　Graziani, G.; Berni, M.; Gambardella, A.; De Carolis, M.; Maltarello, M.C.; Boi, M.; Carnevale, G.; Bianchi, M. Fabrication and characterization of biomimetic hydroxyapatite thin films for bone implants by direct ablation of a biogenic source. *Mater. Sci. Eng. C Mater. Biol. Appl.* **2019**, *99*, 853–862. [CrossRef] [PubMed]

13.　Graziani, G.; Boi, M.; Bianchi, M. A review on ionic substitutions in hydroxyapatite thin films: Towards complete biomimetism. *Coatings* **2018**, *8*. [CrossRef]

14.　Hayami, T.; Hontsu, S.; Higuchi, Y.; Nishikawa, H.; Kusunoki, M. Osteoconduction of a stoichiometric and bovine hydroxyapatite bilayer-coated implant. *Clin. Oral Implant. Res.* **2011**, *22*, 774–776. [CrossRef]

15.　Mihailescu, N.; Stan, G.E.; Duta, L.; Chifiriuc, M.C.; Bleotu, C.; Sopronyi, M.; Luculescu, C.; Oktar, F.N.; Mihailescu, I.N. Structural, compositional, mechanical characterization and biological assessment of bovine-derived hydroxyapatite coatings reinforced with MgF_2 or MgO for implants functionalization. *Mater. Sci. Eng. C Mater. Biol. Appl.* **2016**, *59*, 863–874. [CrossRef]

16. Hashimoto, Y.; Kusunoki, M.; Hatanaka, R.; Hamano, K.; Nishikawa, H.; Hosoi, Y.; Hontsu, S.; Nakamura, M. Improvement of hydroxyapatite deposition on titanium dental implant using ArF laser ablation: Effect on osteoblast biocompatibility in vitro. *Adv. Sci. Technol.* **2006**, *49*, 282–289. [CrossRef]

17. Barinov, S.M.; Fadeeva, I.V.; Ferro, D.; Rau, J.V.; Cesaro, S.N.; Komlev, V.S.; Fomin, A.S. Stabilization of carbonate hydroxyapatite by isomorphic substitutions of sodium for calcium. *Russ. J. Inorg. Chem.* **2008**, *53*, 164–168. [CrossRef]

18. Rau, J.V.; Cesaro, S.N.; Ferro, D.; Barinov, S.M.; Fadeeva, I.V. FTIR study of carbonate loss from carbonated apatites in the wide temperature range. *J. Biomed. Mater. Res. Part B Appl. Biomater.* **2004**, *71*, 441–447. [CrossRef]

19. Supova, M. Substituted hydroxyapatites for biomedical applications: A review. *Ceram. Int.* **2015**, *41*, 9203–9231. [CrossRef]

20. Datta, A.; Gheduzzi, S.; Miles, A.W. A comparison of the viscoelastic properties of bone grafts. *Clin. Biomech.* **2006**, *21*, 761–766. [CrossRef]

21. Figueiredo, M.; Fernando, A.; Martins, G.; Freitas, J.; Judas, F.; Figueiredo, H. Effect of the calcination temperature on the composition and microstructure of hydroxyapatite derived from human and animal bone. *Ceram. Int.* **2010**, *36*, 2383–2393. [CrossRef]

22. Rahavi, S.S.; Ghaderi, O.; Monshi, A.; Fathi, M.H. A comparative study on physicochemical properties of hydroxyapatite powders derived from natural and synthetic sources. *Russ. J. Non-Ferr. Met.* **2017**, *58*, 276–286. [CrossRef]

23. Ramesh, S.; Loo, Z.Z.; Tan, C.Y.; Chew, W.J.K.; Ching, Y.C.; Tarlochan, F.; Chandran, H.; Krishnasamy, S.; Bang, L.T.; Sarhan, A.A.D. Characterization of biogenic hydroxyapatite derived from animal bones for biomedical applications. *Ceram. Int.* **2018**, *44*, 10525–10530. [CrossRef]

24. Figueiredo, M.; Henriques, J.; Martins, G.; Guerra, F.; Judas, F.; Figueiredo, H. Physicochemical characterization of biomaterials commonly used in dentistry as bone substitutes-comparison with human bone. *J. Biomed. Mater. Res. Part B Appl. Biomater.* **2010**, *92b*, 409–419. [CrossRef]

25. de Dios Teruel, J.; Alcolea, A.; Hernandez, A.; Ruiz, A.J. Comparison of chemical composition of enamel and dentine in human, bovine, porcine and ovine teeth. *Arch. Oral Biol.* **2015**, *60*, 768–775. [CrossRef] [PubMed]

26. Haugen, H.J.; Lyngstadaas, S.P.; Rossi, F.; Perale, G. Bone grafts: Which is the ideal biomaterial? *J. Clin. Periodontol.* **2019**, *46*, 92–102. [CrossRef]

27. Sprio, S.; Fricia, M.; Maddalena, G.F.; Nataloni, A.; Tampieri, A. Osteointegration in cranial bone reconstruction: A goal to achieve. *J. Appl. Biomater. Funct. Mater.* **2016**, *14*, e470–e476. [CrossRef]

28. Taschieri, S.; Del Fabbro, M.; Panda, S.; Goker, F.; Babina, K.S.; Tampieri, A.; Mortellaro, C. Prospective clinical and histologic evaluation of alveolar socket healing following ridge preservation using a combination of hydroxyapatite and collagen biomimetic xenograft versus demineralized bovine bone. *J. Craniofacial Surg.* **2019**, *30*, 1089–1094. [CrossRef]

29. Aerssens, J.; Boonen, S.; Lowet, G.; Dequeker, J. Interspecies differences in bone composition, density, and quality: Potential implications for in vivo bone research. *Endocrinology* **1998**, *139*, 663–670. [CrossRef]

30. Akram, M.; Ahmed, R.; Shakir, I.; Ibrahim, W.A.W.; Hussain, R. Extracting hydroxyapatite and its precursors from natural resources. *J. Mater. Sci.* **2014**, *49*, 1461–1475. [CrossRef]

31. Buddhachat, K.; Klinhom, S.; Siengdee, P.; Brown, J.L.; Nomsiri, R.; Kaewmong, P.; Thitaram, C.; Mahakkanukrauh, P.; Nganvongpanit, K. Elemental analysis of bone, teeth, horn and antler in different animal species using non-invasive handheld X-ray fluorescence. *PLoS ONE* **2016**, *11*, e0155458. [CrossRef] [PubMed]

32. Nganvongpanit, K.; Brown, J.L.; Buddhachat, K.; Somgird, C.; Thitaram, C. Elemental analysis of Asian elephant (*Elephas maximus*) teeth using X-ray fluorescence and a comparison to other species. *Biol. Trace Elem. Res.* **2016**, *170*, 94–105. [CrossRef] [PubMed]

33. Surmenev, R.A. A review of plasma-assisted methods for calcium phosphate-based coatings fabrication. *Surf. Coat. Technol.* **2012**, *206*, 2035–2056. [CrossRef]

34. Allaveisi, F.; Mirzaei, M. Effects of high-dose gamma irradiation on tensile properties of human cortical bone: Comparison of different radioprotective treatment methods. *J. Mech. Behav. Biomed. Mater.* **2016**, *61*, 475–483. [CrossRef]

35. Godette, G.A.; Kopta, J.A.; Egle, D.M. Biomechanical effects of gamma irradiation on fresh frozen allografts in vivo. *Orthopedics* **1996**, *19*, 649–653. [CrossRef]

36. Nguyen, H.; Cassady, A.I.; Bennett, M.B.; Gineyts, E.; Wu, A.; Morgan, D.A.; Forwood, M.R. Reducing the radiation sterilization dose improves mechanical and biological quality while retaining sterility assurance levels of bone allografts. *Bone* **2013**, *57*, 194–200. [CrossRef]

37. Nguyen, H.; Morgan, D.A.; Forwood, M.R. Sterilization of allograft bone: Effects of gamma irradiation on allograft biology and biomechanics. *Cell Tissue Bank* **2007**, *8*, 93–105. [CrossRef]

38. Castro-Cesena, A.B.; Sanchez-Saavedra, M.P.; Novitskaya, E.E.; Chen, P.Y.; Hirata, G.A.; McKittrick, J. Kinetic characterization of the deproteinization of trabecular and cortical bovine femur bones. *Mater. Sci. Eng. C Mater. Biol. Appl.* **2013**, *33*, 4958–4964. [CrossRef]

39. Hamed, E.; Novitskaya, E.; Li, J.; Chen, P.Y.; Jasiuk, I.; McKittrick, J. Elastic moduli of untreated, demineralized and deproteinized cortical bone: Validation of a theoretical model of bone as an interpenetrating composite material. *Acta Biomater.* **2012**, *8*, 1080–1092. [CrossRef]

40. Hamed, E.; Novitskaya, E.; Li, J.; Jasiuk, I.; McKittrick, J. Experimentally-based multiscale model of the elastic moduli of bovine trabecular bone and its constituents. *Mater. Sci. Eng. C Mater. Biol. Appl.* **2015**, *54*, 207–216. [CrossRef]

41. Uklejewski, R.; Winiecki, M.; Musielak, G.; Tokłowicz, R. Effectiveness of various deproteinization processes of bovine cancellous bone evaluated via mechano-biostructural properties of produced osteoconductive biomaterials. *Biotechnol. Bioprocess Eng.* **2015**, *20*, 259–266. [CrossRef]

42. ISO 11137-2:2013 Sterilization of Health Care Products—Radiation—Part 2: Establishing the Sterilization Dose. Available online: https://www.iso.org/standard/62442.html (accessed on 27 May 2020).

43. Antonakos, A.; Liarokapis, E.; Leventouri, T. Micro-Raman and FTIR studies of synthetic and natural apatites. *Biomaterials* **2007**, *28*, 3043–3054. [CrossRef] [PubMed]

44. Rehman, I.; Bonfield, W. Characterization of hydroxyapatite and carbonated apatite by photo acoustic FTIR spectroscopy. *J. Mater. Sci. Mater. Med.* **1997**, *8*, 1–4. [CrossRef] [PubMed]

45. Koutsopoulos, S. Synthesis and characterization of hydroxyapatite crystals: A review study on the analytical methods. *J. Biomed. Mater. Res.* **2002**, *62*, 600–612. [CrossRef] [PubMed]

46. Tao, J. FTIR and Raman studies of structure and bonding in mineral and organic-mineral composites. *Methods Enzym.* **2013**, *532*, 533–556. [CrossRef]

47. Al-Akhras, M.A.H.; Qaseer, M.K.H.; Albiss, B.A.; Alebrhim, M.A.; Gezawa, U.S. Investigation of composition and structure of spongy and hard bone tissue using FTIR spectroscopy, XRD and SEM. In *IOP Conference Series: Materials Science and Engineering*; IOP Publishing: Bristol, UK, 2018; Volume 305.

48. Rey, C.; Combes, C.; Drouet, C.; Glimcher, M.J. Bone mineral: Update on chemical composition and structure. *Osteoporos. Int.* **2009**, *20*, 1013–1021. [CrossRef]

49. Sohn, H.S.; Oh, J.K. Review of bone graft and bone substitutes with an emphasis on fracture surgeries. *Biomater. Res.* **2019**, *23*, 9. [CrossRef]

50. Cook, E.A.; Cook, J.J. Bone graft substitutes and allografts for reconstruction of the foot and ankle. *Clin. Podiatr. Med. Surg.* **2009**, *26*, 589–605. [CrossRef]

51. Sousa, S.B.; Castro-Silva, I.I.; da Rocha Coutinho, L.A.C.; Lenharo, A.; Granjeiro, J.M. Osteoconduction and bioresorption of bone allograft versus anorganic bovine bone xenograft: A histomorphometric study in humans. *J. Biomim. Biomater. Tissue Eng.* **2013**, *18*, 85–95. [CrossRef]

52. Rhodes, J.; Mansour, A.; Frickman, A.; Pritchard, B.; Flynn, K.; Pan, Z.; Chang, F.; Miller, N. Comparison of allograft and bovine xenograft in calcaneal lengthening osteotomy for flatfoot deformity in cerebral palsy. *J. Pediatr. Orthop.* **2017**, *37*, e202–e208. [CrossRef]

53. Kubler, N.; Reuther, J.; Kirchner, T.; Priessnitz, B.; Sebald, W. Osteoinductive, morphologic, and biomechanical properties of autolyzed, antigen-extracted, allogeneic human bone. *J. Oral Maxillofac. Surg.* **1993**, *51*, 1346–1357. [CrossRef]

54. Pelker, R.R.; Friedlaender, G.E.; Markham, T.C. Biomechanical properties of bone allografts. *Clin. Orthop. Relat. Res.* **1983**, *174*, 54–57. [CrossRef]

55. Poumarat, G.; Squire, P. Comparison of mechanical properties of human, bovine bone and a new processed bone xenograft. *Biomaterials* **1993**, *14*, 337–340. [CrossRef]

56. Dorozhkin, S.V. Calcium orthophosphate coatings, films and layers. *Prog. Biomater.* **2012**, *1*, 1. [CrossRef] [PubMed]

57. Pu'ad, N.M.; Koshy, P.; Abdullah, H.Z.; Idris, M.I.; Lee, T.C. Syntheses of hydroxyapatite from natural sources. *Heliyon* **2019**, *5*, e01588. [CrossRef]

58. Porter, A.; Patel, N.; Brooks, R.; Best, S.; Rushton, N.; Bonfield, W. Effect of carbonate substitution on the ultrastructural characteristics of hydroxyapatite implants. *J. Mater. Sci. Mater. Med.* **2005**, *16*, 899–907. [CrossRef]

59. Schmidt, C.; Ignatius, A.A.; Claes, L.E. Proliferation and differentiation parameters of human osteoblasts on titanium and steel surfaces. *J. Biomed. Mater. Res.* **2001**, *54*, 209–215. [CrossRef]

60. Gambardella, A.; Berni, M.; Graziani, G.; Kovtun, A.; Liscio, A.; Russo, A.; Visani, A.; Bianchi, M. Nanostructured Ag thin films deposited by pulsed electron ablation. *Appl. Surf. Sci.* **2019**, *475*, 917–925. [CrossRef]

61. de Peppo, G.M.; Agheli, H.; Karlsson, C.; Ekstrom, K.; Brisby, H.; Lenneras, M.; Gustafsson, S.; Sjovall, P.; Johansson, A.; Olsson, E.; et al. Osteogenic response of human mesenchymal stem cells to well-defined nanoscale topography in vitro. *Int. J. Nanomed.* **2014**, *9*, 2499–2515. [CrossRef]

62. Hou, Y.; Yu, L.; Xie, W.; Camacho, L.C.; Zhang, M.; Chu, Z.; Wei, Q.; Haag, R. Correction to surface roughness and substrate stiffness synergize to drive cellular mechanoresponse. *Nano Lett.* **2020**, *20*, 4059. [CrossRef]

63. Prosolov, K.A.; Belyavskaya, O.A.; Linders, J.; Loza, K.; Prymak, O.; Mayer, C.; Rau, J.V.; Epple, M.; Sharkeev, Y.P. Glancing angle deposition of Zn-doped calcium phosphate coatings by RF Magnetron Sputtering. *Coatings* **2019**, *9*, 220. [CrossRef]